Advances in Frontier Research on Engineering Structures
A. Cheshmehzangi and H. Bilgin (Eds.)

doi:10.3233/ATDE230196

Deformation Characteristics and Control Methods of Deep Foundation Pit Excavation in Watery Sandy Soil Area

Wenjie LIU[a, b], Yequan ZHAN[c], Shuang ZHENG[a, b], Jichao LI[d, e], Yunjun QIU[d, e], Dong WEI[a, b], Chao LIU[c, 1]
[a] China Construction Fourth Engineering Bureau Co., Ltd, Guangzhou 510610, China
[b] China Construction Fourth Engineering Bureau Civil Engineering Co., Ltd, Shenzhen 518023, China
[c] School of Civil Engineering, Guangzhou University, Guangzhou 510006, China
[d] China construction infrastructure Co., Ltd, Beijing 100000, China
[e] CSCEC Southern Investment Co., Ltd, Shenzhen 518101, China

Abstract. This paper investigates the deformation characteristics and control methods of support structures during deep foundation pit excavation, using the foundation pit at the Diejiao Station of Foshan Metro Line 3 as a case study. A 3D nonlinear finite element software is employed for excavation simulation, adopting coupled pore fluid diffusion and stress analysis. The numerical model is verified by comparing the field monitoring data with the finite element results. The study systematically analyzes the influence of reinforcement position, reinforcement parameters, and reinforcement depth on the maximum lateral displacement of the diaphragm wall of the foundation pit. The research results reveal that reinforcing the soil on both sides of the diaphragm wall can effectively reduce the lateral deformation of the foundation pit. Furthermore, the study shows that external reinforcement of the diaphragm wall can reduce the maximum lateral displacement of the wall to a certain extent, but the reinforcement effect is limited. The reinforcement effect of the inner side of the diaphragm wall improves with the increase of the excavation depth. Properly increasing the Young's modulus of the reinforcement can reduce the adverse effect of excavation on the foundation pit. Finally, the optimal depth of reinforcement is found to be the excavation depth of the foundation pit of 28.2m. The research results can provide a reference for the foundation pit reinforcement scheme in watery sandy soil areas.

Keywords. foundation pit excavation, finite element analysis, support deformation characteristics, reinforcement parameters

1. Introduction

With the rapid development of urbanization, the construction of metro stations has brought about a large number of deep foundation pit engineering problems. Especially in urban construction of metro pits, the deformation of its enclosure structure and its impact on the surrounding environment are often the main issues to be considered in the

[1] Corresponding author: Chao LIU, School of Civil Engineering, Guangzhou University, Guangzhou 510006, China; e-mail: chaoliu@gzhu.edu.cn

design of deep pit support [1]. Jin et al. [2] used numerical analysis and immovable point adjustment coefficient calculation methods to calculate the forces on the foundation support structure under different types of asymmetric loads. They proposed that reinforcement of the weak side foundation can effectively reduce the deformation of the support structure caused by the imbalance of soil pressure on both sides, and concluded in [3] that the depth and width of the slot wall reinforcement are the key factors affecting the stability of the reinforcement. Under the premise that the depth and width of the reinforcement meet the safety of stability, the wider the reinforcement, the smaller its depth, and conversely, the longer the reinforcement, the narrower its width. Yang et al. [4] showed that MJS piles can effectively reduce the impact of foundation excavation on the surrounding environment by increasing the Young's modulus, pile length, and diameter of MJS piles. Designing MJS piles as end-bearing piles can significantly reduce the surface settlement and deformation of diaphragm walls. Wang et al. [5] showed that soil reinforcement in the active compression zone of a foundation pit can be controlled by applying reinforcement at the location of maximum lateral deformation of the wall. They also suggested that the maximum lateral deformation of the wall can be limited by increasing the thickness of the diaphragm wall on the stressed side.

Based on the above study, it can be seen that the excavation greatly influences the surrounding environment of the pit, and the support structure plays an important role in suppressing the deformation of the pit. The excavation depth of 25.64m represents a typical case of a deep foundation pit with a water-rich sandy soil stratum in South China, and can provide a reference for studying deformation characteristics and support structures of similar deep foundation pit projects with thick sandy soil layers. The 3D finite element analysis model considers the effect of pore water on the excavation process and compares the monitoring data with the numerical results in the west area to verify the correctness of the numerical model, followed by a parametric study. The obtained conclusions provide reasonable optimization suggestions for the excavation of the eastern part of the Diejiao station.

2. Project Overview

2.1. Diejiao Metro Station

Diejiao station is one of the stations on Line 3 of the Foshan Metro, situated at the intersection of Wenhua North Road, Hai San Road, and Wenchang Road. It is an underground three-story stacked line side station with a total length of 149.8m, a standard section width of 35.9m, and an expanded end width of 38.7m. The main structure was constructed using the open cut smooth method, as shown in Figure 1.

The foundation pit support design uses a 1000mm thick diaphragm wall and four concrete internal supports. The wall depth is 30m, and both sides of the diaphragm wall are reinforced with Φ850 mixing piles. The diameter of the precipitation well pipe is 1.2m, and the well depth is 30m.

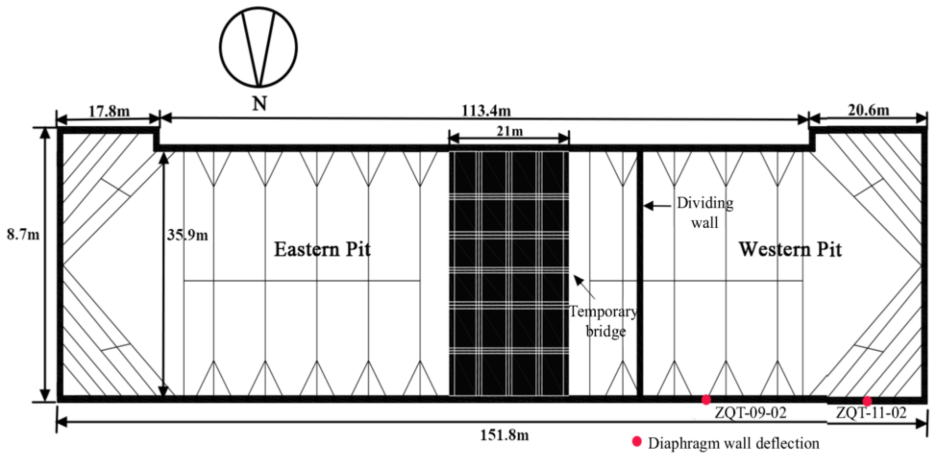

Figure 1. Layout of foundation pit

2.2. Geological Conditions

The distribution of soil layers at this station is shown in Figure 2, where the <2-2> silty fine sand layer and <3-2> medium coarse sand layer are the main soil layers encountered during excavation. The base slab is primarily located in the <7-2> strongly weathered rock layer, and the end of the diaphragm wall is primarily located in the <8-2> medium weathered rock layer. Furthermore, the static groundwater level is shallow, with an average burial depth of 1.0m.

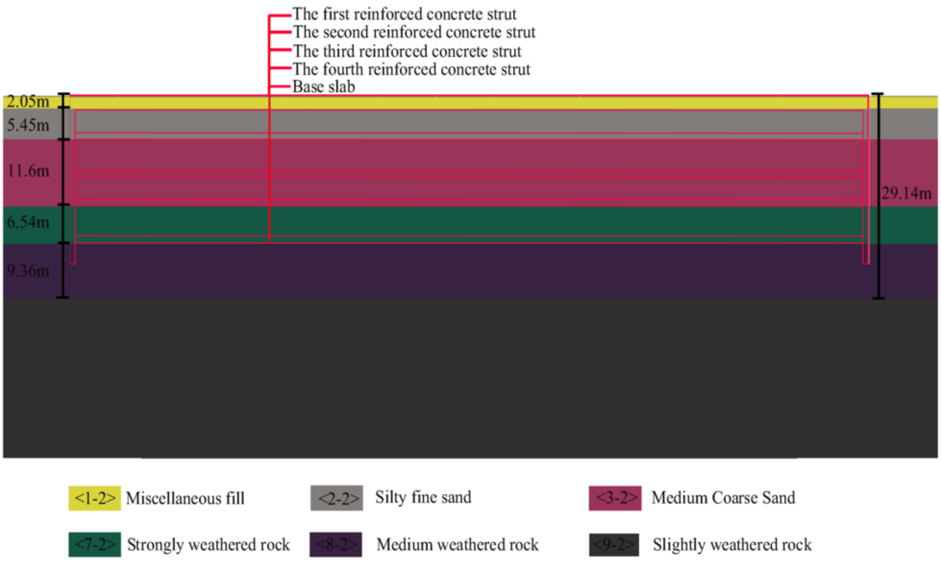

Figure 2. Soil profile diagram

3. FEA Model

3.1. Geometry and Material

In this paper, a three-dimensional numerical model of the project is established using ABAQUS. The zone of influence of foundation excavation proposed by Hsieh. P.G and Ou C.Y [6] suggests that a distance of 4 times the depth of excavation behind the diaphragm wall will be influenced by excavation. Therefore, the model size in this paper is 455 m (length) x 220 m (width) x 99.7 m (height), (as shown in Figure 3), which satisfies the requirement that the boundary conditions have no effect on the pit deformation. The boundary conditions for the model include displacement constraints in all directions at the bottom and zero normal phase displacements on all four sides. A 20 kPa overload was applied to the ground and to the working surface at each step to simulate the ground yard and additional working loads, and the gravity was applied uniformly throughout the model. Additional vehicle loads of 27 kPa were applied to the temporary bridge according to the design requirements [7]. The method proposed by Xu J.B [8] and Dong Dang [9] was used to calculate the additional vehicle loads.

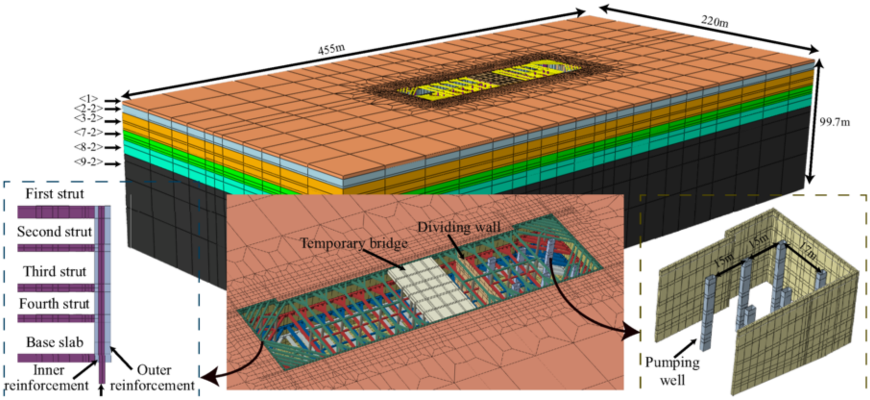

Figure 3. Finite element model

Considering the influence of pore water pressure on the simulation, the pore water pressure boundary at the ground surface is set to zero before the foundation pit is excavated. According to the principle of area equivalence of permeable surfaces, the circular section precipitation well was converted into a square section with a side length of 0.9 m [10]. The well was set up with permeable surfaces around the perimeter and impermeable surfaces at the bottom. The groundwater level is kept below the excavation surface at all times during excavation, and a constant head boundary is defined on the soil grid in contact with the precipitation well. Zero head is defined in the depth range above the working surface, and a linear distribution of hydrostatic pressure head is defined in the range below the working surface.

Ou C.Y et al. [11] proposed three options for soil reinforcement, namely block type, column type and wall type, Li D.Y et al. [12] compared the three options and proposed that the block type has a better reinforcement effect. Therefore, this paper uses the block reinforcement scheme.

The Modified Cam-Clay (MCC) model is used for the silty fine sand layer (Layer 2-2), while the Mohr-Coulomb (MC) model is used for the other soil layers. According to the literature [13]-[15], soil reinforcement is modeled using linear elastic material with a modulus of elasticity of 300 MPa and Poisson's ratio of 0.2. The model assumes elastic materials for the drop shaft, base slab, support system, and central column. As the interaction between the soil and the diaphragm wall is face-to-face contact based on Coulomb friction, the friction coefficients of the soil layers from top to bottom are 0.25, 0.3, 0.4, 0.45, and 0.5, respectively. The detailed material parameters are listed in Table 1.

Table 1. Material properties in FEA

Soil layer	γ (kN/m^3)	M	λ	κ	υ	e_1	k (m/s)	K	c' (*kPa*)	φ' (°)	E (MPa)
<1>	**16.2**				**0.35**		1.16×10^{-5}		**10**	**15**	**12**
<2-2>	**19.2**	**1.2**	**0.047**	**0.007**	**0.33**	**0.927**	1.16×10^{-7}	**0.78**			
<3-2>	**18.5**				**0.25**		1.39×10^{-4}		**5**	**32**	**20**
<7-2>	**20.0**				**0.25**		5.79×10^{-6}		**50**	**29**	**80**
<8-2>	**21.0**				**0.2**		1.74×10^{-6}		**180**	**32**	**1000**
<9-2>	**22.0**				**0.2**		5.79×10^{-7}		**350**	**39**	**2500**

γ: unit weight; M: stress ratio; λ: logarithmic plastic bulk modulus; κ: logarithmic bulk modulus; υ: Poisson's ratio; e_1: intercept of virgin consolidation line in $e - \ln p'$; k: permeability coefficient; K: flow stress ratio; c': effective cohesion; φ': effective friction angle; and E: Young's modulus.

3.2. Simulation Procedure

The excavation simulation uses 'element death' techniques to simulate the parts of the model that need to be removed or imposed by deactivating or reactivating elements. The construction time is set according to the daily construction schedule, and the groundwater level is kept below the excavation surface at all times during the excavation. The excavation simulation process is presented in Table 2.

Table 2. Excavation simulation process

Step	Interval (Day)	Date (yyyy/mm/dd)	Construction activities
0			Initialization is conducted
1	60	2020/9/20~2020/11/21	Diaphragm walls, soil reinforcement, drop shafts and 30 columns are constructed
2	18	2020/12/13~2021/1/23	The first strut and temporary bridge are installed
3	14	2021/2/23~2021/3/9	Excavation to the depth 6.3 m
4	5	2021/3/11~2021/3/16	The second strut in the excavation surface is installed
5	14	2021/3/17~2021/3/30	Excavation to the depth 12.8 m
6	8	2021/3/31~2021/4/7	The third strut in the excavation surface is installed
7	10	2021/4/8~2021/4/17	Excavation to the depth 17.8 m
8	7	2021/4/18~2021/4/24	The fourth strut in the excavation surface is installed
9	27	2021/4/25~2021/5/29	Excavation to the depth 25.64 m. The base slab is installed

3.3. Validation of the Model

Figure 4 shows the monitored and simulated deflection values of the diaphragm wall at ZQT-09-02 and ZQT-11-02 during the excavation. It can be observed from the figure that the location, maximum value, and deformation trend of the diaphragm wall are in good agreement between the simulated and monitored values. The deformation curve is bow-shaped, with smaller values at both ends and larger values in the middle, and the lateral displacement of the wall increases as the excavation depth increases. Moreover, the position of the maximum horizontal wall displacement moves progressively downwards, which is consistent with the typical lateral deformation pattern of embedded rock walls [16].

The difference between the monitored and simulated values is insignificant and can be attributed to minor seepage in the pit. Moreover, the north side of the pit serves as a yard where heavy construction equipment such as excavators and cranes operate, leading to additional active earth pressure on the diaphragm wall and thereby amplifying its lateral movement.

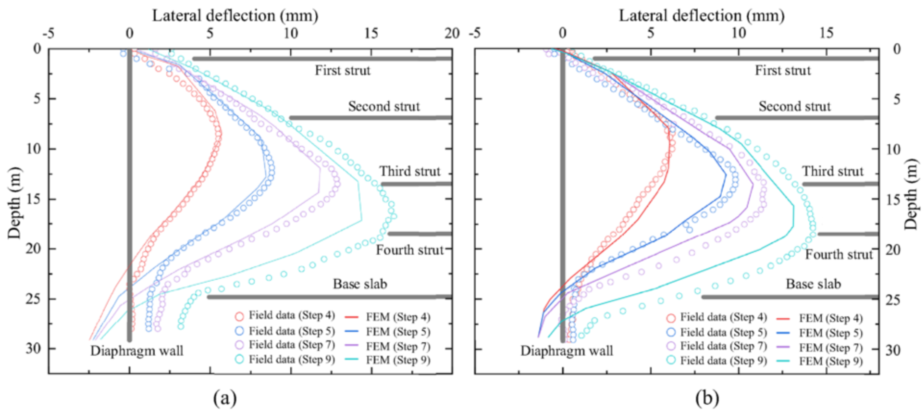

Figure 4. Comparison of FEM results and field data for wall deflection: (a) ZQT-09-02; (b) ZQT-11-02

To further investigate the performance of deep foundation excavation in sandy soil areas, the maximum lateral displacement of the diaphragm wall was plotted against the depth of excavation based on the monitored and simulated values and compared with the results from other sandy soil areas, as shown in Figure 5. As can be seen from the figure, the ratio of maximum lateral deflection to excavation depth δ_{hm}/H measured in this case ranged from 0.051% to 0.205%, with an average value of approximately 0.995%. Li et al. (2014) [17] and Dellari (2016) [18] monitored the lateral deformation of diaphragm walls in deep excavations with sand-rich and clay-rich soils in Shenzhen and Chicago, respectively. Hsiung et al. (2016) [19] used numerical simulation to obtain the effect of wall deformation in a pit containing loose sand layers in Taiwan; and Elbaz et al. (2018) [20] analyzed the case of a typical sandy soil pit in Guangzhou. The comparative analysis found that the δ_{hm}/H of all these cases ranged from 0.051% to 0.205%.

In summary, the numerical simulation results agree well with the monitoring data, verifying the feasibility of the simulation approach for this case. Further investigations can be conducted based on this study.

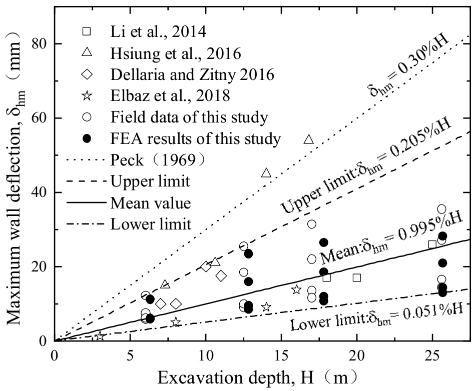

Figure 5. Relationship between maximum lateral displacement of diaphragm wall and excavation depth

4. Discussions

To investigate the impact of reinforcement on excavation, we employed the aforementioned model as the baseline model, denoted as RM (Reinforced Model). Based on model RM, we established two additional models: one without any reinforcement for the foundation pit, denoted as M (Unreinforced Model), and two others with reinforcement applied solely to the outer and inner sides of the wall, respectively, designated as RMO (Reinforced Model with Outer reinforcement) and RMI (Reinforced Model with Inner reinforcement).

This paper examines several parameters of the reinforcement, including its position, Young's modulus, and depth. The impact of Young's modulus is assessed by adjusting the multiplication factor k_e, such as $k_e E_0$, where E_0 represents the initial Young's modulus of the reinforcement. Table 3 outlines the specifics of the parameter study. The parameter R, which characterizes the effect of reinforcement, is defined as follows:

$$R = (\omega_M - \omega_{RM})/\omega_M \tag{1}$$

Where ω_M is the maximum value of the M model (settlement or deflection) and ω_{RM} is the maximum value of the reinforcement model.

Table 3. Summary of parametric study

No.	Reinforcement position	Multiplication factor of reinforcement modulus k_e	Reinforcement depth L (m)
1	outer side, inner side, both side	1	29.14
2	both side	0.4, 0.6, 0.8, 1, 1.5, 2	29.14
3	both side	1	6.3, 12.8, 17.8, 25.6, 29.14

4.1. Influence of Different Reinforcement Position

Figure 6 illustrates that the presence of inner reinforcement has a significant impact on the deflection of the diaphragm wall, and the reinforcement effect increases as the depth of excavation deepens. This is because the inner reinforcement effectively mitigates the impact of seepage on the wall and improves the water stopping curtain effect of the diaphragm wall. At a depth of 16 m, the impact of the inner reinforcement is comparable to, or even surpasses, that of the reinforcement on both sides. This is because the area at this depth is predominantly rocky, and the strength of the rock is higher than that of the reinforcement, causing the outer reinforcement to have a negative effect. Moreover, the inner reinforcement prevents the ground outside the wall from settling, especially in favorable geological conditions, and the reinforcement effect becomes increasingly pronounced.

The impact of outer reinforcement on the deflection of the diaphragm wall is minor, whereas its effect on the settlement of the ground outside the wall is significant and gradually diminishes as the excavation depth increases. This is because the outer reinforcement primarily controls the deformation caused by the deformation of the supporting structure by obstructing the pathways that affect the deformation of the outer soil, thereby mitigating the impact on the surrounding environment, but it has limited control over the deformation of the supporting structure itself. Reinforcement on both sides can notably reduce the lateral deformation of the wall and suppress the surface settlement behind the wall, but the effect of suppressing wall deformation decreases when the excavation reaches 14.1 m, while the degree of surface settlement suppression gradually decreases with the increase of excavation depth. This is due to the fact that the upper soil layer predominantly consists of soft soils such as silty silt, with high compressibility, and the excavation unloading has a greater impact on the diaphragm wall and the soil outside the wall, making the reinforcement effect relatively favorable. This underscores the necessity of reinforcing diaphragm walls in clayey sandy soil areas.

In summary, in soft soil excavations with limited project budgets, priority should be given to reinforcing both sides of the wall. However, for excavations with better soil conditions, only the inner side needs to be reinforced.

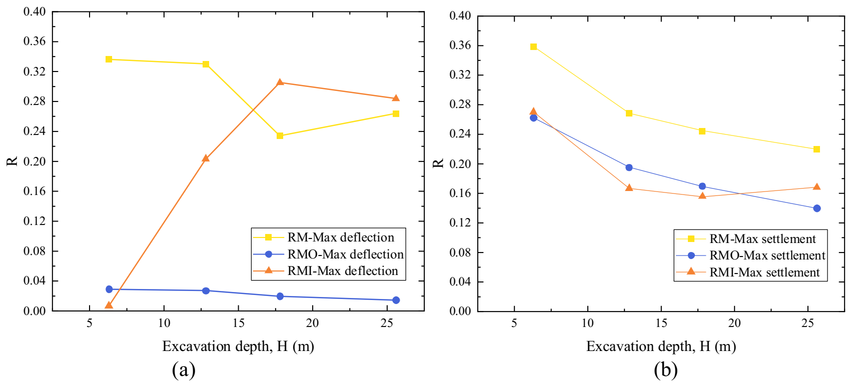

Figure 6. Influence of reinforcement position: (a) Max deflection; (b) Max settlement

4.2. Influence of Young's Modulus of Reinforcement

As shown in Figure 7, the reinforcement effect decreases with increasing excavation depth, especially concerning the settlement of the ground outside the wall. Secondly, as the reinforcement modulus increases, both the maximum lateral displacement of the wall and the ground settlement decrease. When k_e increases from 0.8 to 1.0, the difference in R-value of maximum wall deflection is between 0 to 0.03, and the R-value of maximum ground settlement remains within 0.02 of the difference. This suggests that both wall deflection and ground settlement are relatively stable when k_e is greater than 0.8. Therefore, in actual construction, the excavation's impact on the support structure and the surrounding area can be controlled by selecting a reinforcement with adequate strength while considering the project's cost.

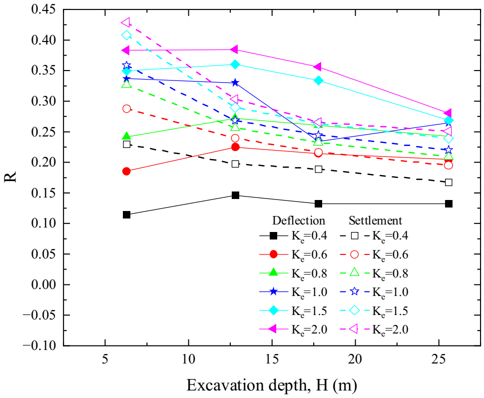

Figure 7. Influence of Young's modulus of reinforcement

4.3. Influence of Depth of Reinforcement

As shown in Figure 8, the depth of reinforcement has a significant effect on both the maximum lateral deflection of the diaphragm wall and the maximum post-wall ground settlement. The wall deflection and ground settlement decrease gradually with increasing depth, but as the depth increases from 25.6 m to 29.14 m, the R-value of the diaphragm wall deflection becomes smaller and fluctuates more depending on the depth. For excavations in the central soil layer, which is soft sandy soil, a reinforcement depth of 29.14 m is more effective than 25.6 m in controlling the ground settlement outside the wall. This is because a longer reinforcement depth can more effectively control the water linkage between the internal and external groundwater, reduce the impact of pit precipitation on the soil outside the wall, and thus reduce surface settlement.

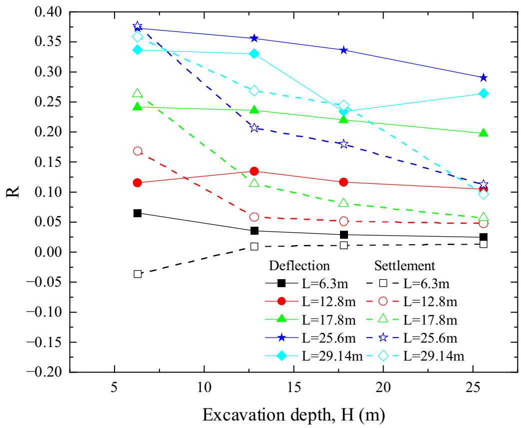

Figure 8. Influence of depth of reinforcement

Zhang W.C et al. [21] combined Coulomb's earth pressure theory to calculate a reasonable width for the reinforcement zone. When there is sufficient space on the outer side of the foundation pit, the width of the reinforcement zone W can be determined using Equation (2):

$$W = h\tan(\varphi'/2) \tag{2}$$

Where h is the reinforcement depth and φ' is the effective internal friction angle. When space on the outside of the pit is limited, a smaller reinforcement width is used, and the reinforcement depth is appropriately increased to 1.0H to 1.2H. Therefore, in this case, a reinforcement depth of 1.1H (i.e., 28.2 m) can be used to economically and effectively reduce deformation of the support structure and surrounding soil, taking into account the limited space on the outside of the pit and selecting a suitable smaller reinforcement width.

5. Conclusions

- Reinforcement of both sides of the wall during excavation in soft soil layers can efficiently reduce the deformation of the diaphragm wall and thus improve the overall stability of the pit. In excavations with good geological conditions or where the surrounding environment does not allow for reinforcement, the option of reinforcing only the inner side can be used to obtain the most economical and effective reinforcement solution.
- The increase in the Young's modulus of the reinforcement is effective in controlling the deformation of the pit. However, there is a limit to the effect of the deformation inhibition, which ceases to increase beyond a certain level of reinforcement strength.
- An appropriate depth of reinforcement can effectively control the linkage between internal and external groundwater, thereby reducing surface settlement. Based on the study findings, a reinforcement depth of 1.1 H (i.e., 28.2 m) is recommended as the optimal depth.

Acknowledgements

The research was conducted with funding provided by National Science Foundation of China (No. 52178385), Science and Technology Program of Guangzhou, China (No. 202102020617 and No. 202201020171).

References

[1] J.H. Liu, X.Y. Hou. Foundation excavation engineering manual[M]. Architecture & Building Press, Beijing: China, 1997.
[2] Y.B. Jin, D. Liu, Y. Sun. Design and Calculation Method of Inner Support Structure in Deep Foundation Pit under Asymmetric Load[J]. Chinese Journal of Underground Space and Engineering, 2019, 15(06): 1811-1818.
[3] Y.B. Jin. A method for determination of reinforcement width and depth of trench face of diaphragm wall[J]. Rock and Soil Mechanics, 2017, 38(S2): 273-278.

[4] Y.B. Yang, J.S. Li, C. Liu et al. Influence of deep excavation on adjacent bridge piles considering underlying karst cavern: a case history and numerical investigation[J]. Acta Geotechnica, 2021: 1-18.
[5] K.Y. Wang et al. Lateral Deformation Characteristics and Control Methods of Foundation Pits Subjected to Asymmetric Loads[J]. Symmetry, 2021, 13(3): 476-476.
[6] P.G. Hsieh, C.Y. Ou. Simplified Approach to Estimate the Maximum Wall Deflection for Deep Excavations with Cross Walls in Clay Under the Undrained Condition[J]. Acta Geotech, 2015, 11(1): 177-189.
[7] People's Traffic Press. General Specification for the Design of Highway Bridges and Culverts: JTG D60-2004. [S]. Beijing: People's Transport Publishing House, 2004: 74-76.
[8] J.B. Xu, M.T. Liu. Analytical study on the value of the action of automobile load on underground structures[J]. Urban Roads and Bridges and Flood Control, 2019, (5): 301-304, 34.
[9] D. Dang. Research on design loads and their combinations for highway bridges [D]. Chang'an University, 2012.
[10] C. Li. Numerical simulation of vertical well precipitation based on ABAQUS [D]. Tianjin University, 2008.
[11] C.Y. Ou, T.S. Wu, H.S. Hsieh. Analysis of Deep Excavation with Column Type of Ground Improvement in Soft Clay[J]. American Society of Civil Engineers (Asce), 1996, 122(9): 709-716.
[12] D.Y. Li, X.N. Gong, T.Q. Zhang. Numerical simulation of underground pipeline protection measures around deep foundation pits with soft ground[J], 2001, (6): 736-740.
[13] X.L. Gu, H.J. Qian, H.S. Liu, et al. Foundations and foundations [M]. Construction Industry Press, Beijing: China 2003.
[14] J.J. Li, R.W. Liang. Research on compression strength and modulus of deformation of cemented soil[J]. Rock and Soil Mechanics, 2009, 30(2): 473－477.
[15] J.Q. Ma, Y.X. Wang, H.M. Li et al. Study on the Relations of Cement-Soil Parameters with Compressive Strength[J]. Building Science, 2009, 25(3): 65－67.
[16] Z.Z. He, X. Yang, C. Ye, et al. Optimization analysis of support structures in deep foundation pits for subways[J]. 2021, 28(1): 68-78.
[17] H. Li, S.L. Shen, D.W. Hou, et al. Analysis on Environmental Impact of Deep Excavation in Shenzhen, China[C]. Tunneling and Underground Construction, 2014: 283-292.
[18] J. Dellaria, B. Zitny. Combining Multiple Techniques to Complete an Urban Deep Excavation[C] American Society of Civil Engineers: Geotechnical and Structural Engineering Congress, 2016: 351-364.
[19] B.C.B. Hsiung, K.H. Yang, W. Aila, et al. Three-dimensional Effects of a Deep Excavation on Wall Deflections in Loose to Medium Dense Sands[J]. Computers and Geotechnics, 2016, 80: 138-151.
[20] K. Elbaz, S. Shen, Y. Tan, et al. Investigation Into Performance of Deep Excavation in Sand Covered Karst: a Case Report[J]. Soils and Foundations, 2018, 58(4): 1042-1058.
[21] W.C. Zhang, W. Xue, F. Yu. Effects of active zone soil reinforcement on deep foundation pits[J]. Journal of Underground Space and Engineering, 2015, 11(S1): 205-210.